

## RESEARCH ARTICLE

# Effectiveness of different pre-treatments in recovering pre-burial isotopic ratios of charred plants

O. Brinkkemper<sup>1</sup>  | F. Braadbaart<sup>2</sup> | B. van Os<sup>1</sup> | A. van Hoesel<sup>1</sup> | A.A.N. van Brussel<sup>3</sup> | R. Fernandes<sup>4,5</sup><sup>1</sup>Cultural Heritage Agency, PO Box 1600, 3800 BP, Amersfoort, The Netherlands<sup>2</sup>Department of Earth Sciences-Geochemistry, Utrecht University, PO Box 80021, 3058 TA, Utrecht, The Netherlands<sup>3</sup>Department of Plant Molecular Biology (Sylvius Laboratories), Leiden University, PO Box 9502, 2300 RA, Leiden, The Netherlands<sup>4</sup>Department of Archaeology, Max Planck Institute for the Science of Human History, Kahlaische Strasse 10, D-07745 Jena, Germany<sup>5</sup>McDonald Institute for Archaeological Research (University of Cambridge), Downing Street, Cambridge CB2 3ER, UK**Correspondence**

O. Brinkkemper, Cultural Heritage Agency, PO Box 1600, 3800 BP Amersfoort, The Netherlands.

Email: o.brinkkemper@cultureelerfgoed.nl

R. Fernandes, Department of Archaeology, Max Planck Institute for the Science of Human History, Kahlaische Strasse 10, D-07745 Jena, Germany.

Email: fernandes@shh.mpg.de; rf385@cam.ac.uk

**Rationale:** Isotopic analysis of archaeological charred plant remains offers useful archaeological information. However, adequate sample pre-treatment protocols may be necessary to provide a contamination-free isotopic signal while limiting sample loss and achieving a high throughput. Under these constraints, research was undertaken to compare the performance of different pre-treatment protocols.**Methods:** Charred archaeological plant material was selected for isotopic analysis ( $\delta^{13}\text{C}$  and  $\delta^{15}\text{N}$  values) by isotope ratio mass spectrometry from a variety of plant species, time periods and soil conditions. Preservation conditions and the effectiveness of cleaning protocols were assessed through Fourier transform infrared spectroscopy and X-ray fluorescence (XRF) spectrometry. An acid–base–acid protocol, successfully employed in radiocarbon dating, was used to define a contamination-free isotopic reference. Acid–base–acid isotopic measurements were compared with those obtained from untreated material and an acid-only protocol.**Results:** The isotopic signals of untreated material and the acid-only protocol typically did not differ more than 1‰ from those of the acid–base–acid reference. There were no significant isotopic offsets between acid–base–acid and acid-only or untreated samples. Sample losses in the acid–base–acid protocol were on average  $50 \pm 17\%$  (maximum = 98.4%). Elemental XRF measurements showed promising results in the detection of more contaminated samples albeit with a high rate of false positives.**Conclusions:** For the large range of preservation conditions described in the study, untreated charred plant samples, water cleaned of sediments, provide reliable stable isotope ratios of carbon and nitrogen. The use of pre-treatments may be necessary under different preservation conditions or more conservative measurement uncertainties should be reported.

## 1 | INTRODUCTION

Carbon and nitrogen stable isotope ratios (in delta notation  $\delta^{13}\text{C}$  and  $\delta^{15}\text{N}$  values) measured in charred plant material obtained from buried contexts represent a valuable source of archaeological information.<sup>1</sup> This includes the reconstruction of past climatic histories and agricultural practices.<sup>2–5</sup> In addition, the isotopic signatures of edible plants are necessary for defining isotopic baselines in isotope-based ancient human diet reconstruction studies.<sup>6</sup> Estimates of pre-charring plant bulk isotopic signals are possible since several experimental studies have quantified the isotopic offsets introduced during the charring process.<sup>7–9</sup> However, diagenetic modifications and the incorporation of foreign contaminants (e.g. carbonates, humic substances) may alter pre-deposition plant isotopic signals.<sup>10</sup> Thus, the use of pre-screening techniques capable of

identifying the presence of contaminants and the use of protocols that remove contaminants may become necessary.<sup>11</sup> The employed protocols should also not alter the original plant isotopic signal by selectively removing endogenous compounds having contrasting isotopic signatures.<sup>4,12–14</sup> Finally, an optimal cleaning protocol should also limit sample loss and allow for a high sample throughput.

Acidification of buried plant samples removes deposited carbonates while an alkali step removes humic acids.<sup>10</sup> The high pH during the alkali step introduces into solution atmospheric  $\text{CO}_2$  and its removal is achieved with an additional acid step.<sup>15</sup> Thus, variants of acid–base–acid (ABA) protocols are often employed in stable isotope and radiocarbon analysis of archaeological plant material.<sup>8,10,16–19</sup> Radiocarbon testing of ABA protocols on charred and uncharred plant material, showing variable preservation conditions and older than 50,000 years ( $^{14}\text{C} \approx 0$ ),

demonstrated that such protocols are capable of achieving an accuracy typically better than 0.5%.<sup>17-19</sup> At this level of accuracy, stable isotope analysis, for usual plant isotopic ratios,<sup>10,12</sup> would provide measurements within typical measurement uncertainty for  $\delta^{13}\text{C}$  values (ca 0.2%). Furthermore, nitrogen and carbon isotope measurements on experimentally charred modern cereal grains treated following an ABA protocol showed random offsets towards uncharred isotope ratios and within measurement uncertainty.<sup>8</sup> Thus, the ABA protocol did not selectively leach plant compounds (e.g. macronutrients, calcium oxalate or phytate, amino acids) having contrasting isotopic signals<sup>4,12,13,20</sup> in sufficient amounts to significantly alter the original bulk signal. However, a main disadvantage of ABA protocols is that they cause large sample losses particularly for powdered samples, and increase the risk of laboratory contamination.<sup>11,16</sup>

Pre-treatment alternatives to an ABA protocol have been employed including acid-only protocols,<sup>5,21-25</sup> acid-only or base-acid protocols following infrared pre-screening,<sup>11</sup> and no pre-treatment.<sup>26,27</sup> Statistical comparison of isotopic ratios from untreated and acid-only pre-treated archaeological samples of single charred grains from the Iron Age site of Danebury Hillfort (UK) showed no significant difference in either  $\delta^{13}\text{C}$  or  $\delta^{15}\text{N}$  values.<sup>21</sup> Other studies have compared the isotopic ratios of untreated and ABA-treated archaeological samples from different locations and time periods.<sup>8,11,16</sup> These studies showed that the  $\delta^{13}\text{C}$  offsets between untreated and ABA-treated samples were random and in 96% of the cases ( $n = 52$ ) up to 1‰. For  $\delta^{15}\text{N}$  values the observed offsets were smaller than 1.5‰ in 96% of the cases. The distribution of  $\delta^{15}\text{N}$  offset values varied with case study: random,<sup>8</sup> elevated  $\delta^{15}\text{N}$  values following ABA<sup>16</sup> and lowered  $\delta^{15}\text{N}$  values following ABA.<sup>11</sup> These results show that the impact of environmental contamination was relatively minor as a probable result of limited addition of exogenous material and comparatively small isotopic differences between endogenous and contaminant material.<sup>28,29</sup> Furthermore, surviving alkali-extractable substances also include endogenous material that underwent diagenetic or thermogenic alteration.<sup>30</sup>

The goal of this study was to test the hypothesis that untreated buried charred plant samples are relatively robust in preserving pre-burial bulk isotopic signals under certain environmental conditions (e.g. soil types, climate). This study expands considerably on previous research by including samples of varied species recovered from sites of different soil types and spanning a wide chronological range. The degree of sample contamination and diagenetic alteration was assessed through measurements of infrared absorption peaks using Fourier transform infrared (FTIR) spectroscopy and through measurements of elemental composition using a portable X-ray fluorescence (p-XRF) device. The isotopic ratios of untreated plant samples were compared with those following acid-only and ABA pre-treatments; the latter was taken as reference for pre-burial bulk isotopic signatures.

## 2 | EXPERIMENTAL

### 2.1 | Materials

Twenty-two different samples of charred plant remains collected from archaeological sites were selected for study from the Dutch archaeobotanical database RADAR.<sup>31</sup> The plant species, number of

grains selected for analysis, sample weight, archaeological site location, site soil type and site chronology are listed in Table 1. The samples were water cleaned of attached sediments following recovery from the archaeological site, and the botanical remains identified and collected in glass or plastic containers by the original archaeobotanical researcher. For the present study, the original identifications were checked under a stereomicroscope (8× to 60× magnification) and the remains were photographed.

### 2.2 | Sample pre-treatments

Sample pre-treatment was carried out at the Sylvius laboratory (Leiden University, The Netherlands). All samples were powdered using a pestle and mortar. Samples were dried for 48 hours at 60°C and weighed with a precision of 0.1 mg immediately after drying. Isotopic analysis was performed for sample aliquots of untreated plant material, material subjected to an acid-only (A-only) protocol and material subjected to an ABA protocol. The employed ABA protocol was as described by Santos and Ormsby for the radiocarbon dating of plant material.<sup>19</sup> This protocol is similar to the ABA protocols employed previously in similar studies for stable isotope analysis.<sup>8,11,13</sup>

The steps for A-only and ABA pre-treatments were as follows:

- Soaking in 1.0 M HCl at 85°C for 30 min
- Rinsing (5 times)
- Drying for 48 h at 60°C and weighing for estimate of acid-only sample loss
- Sample taken for isotopic analysis (A-only protocol)
- Soaking in 1.0 M NaOH at 85°C for 60 min
- Rinsing (5 times)
- Soaking in 1.0 M HCl at 85°C for 30 min
- Rinsing (5 times)
- Drying for 48 h at 60°C and weighing for estimate of base-acid sample loss
- Sample taken for isotopic analysis (ABA protocol)

Each rinsing step consisted of washing using Milli-Q (Millipore, Billerica, MA, USA) ultrapure water (18 M $\Omega$ ) followed by centrifugation (5000 rpm) with a Sorvall RC5B Plus centrifuge in glass tubes. Decantation was performed carefully to limit sample losses. Samples were weighed with a precision of 0.1 mg following A-only and full ABA pre-treatments for estimates of sample loss.

### 2.3 | Stable isotope analysis

Isotopic measurements were performed in duplicate at the Division of Archaeological, Geographical and Environmental Sciences of the University of Bradford (Bradford, UK). Approximately 1–2 mg of charred plant material was weighed into tin capsules for analysis with a Flash EA 1112 organic elemental analyser (Thermo Scientific, Bremen, Germany) coupled to a Thermo Scientific Delta Plus isotope ratio mass spectrometer. Given the considerably lower sample concentration of nitrogen than of carbon, a helium dilution was

**TABLE 1** Description of charred plant samples employed in this study

Sample no.	Species	Number of grains	Dry weight (mg)	Site	Find number	Soil	Latitude (N)	Longitude (E)	Chronology
1	Millet ( <i>Panicum miliaceum</i> )	60	91.4	Deventer Colmschate	62/1/7	Sand	52° 14' 58.8"	6° 12' 27.7"	Early Iron Age (800–500 BC)
2	Emmer ( <i>Triticum dicoccon</i> )	30	364.6	Spijkenisse 10-36	180	Peat	51° 51' 33.6"	4° 17' 11.1"	Roman period (12 BC–AD 450)
3	Emmer ( <i>Triticum dicoccon</i> )	30	206.3	Aartswoud-Mienakker	2880	Marine clay	52° 44' 4.0"	4° 56' 10.5"	Late Neolithic (2800–2400 BC)
4	Breadwheat ( <i>Triticum aestivum</i> )	30	220.9	Deil-Eigenblok	30189	River clay	51° 55' 7.1"	4° 29' 25.1"	Early Bronze Age (2000–1800 BC)
5	Breadwheat ( <i>Triticum aestivum</i> )	30	279.9	Zutphen Stadhuis	5/2-3/957a	River clay	52° 8' 23.8"	6° 11' 41.0"	Early Medieval (AD 700–800)
6	Spelt ( <i>Triticum spelta</i> )	30	435.0	Voerendaal-ten Hove	20-4-25	Loess	50° 52' 59.8"	5° 54' 31.3"	Roman period (AD 100–400)
7	Rye ( <i>Secale cereale</i> )	30	147.5	Raalte-Heeten	11/2/72	Sand	52° 19' 43.9"	6° 16' 54.4"	Roman period (AD 300–450)
8	Rye ( <i>Secale cereale</i> )	30	181.6	Deventer Burseplein	51/2/19	River clay	52° 15' 3.9"	6° 9' 28.0"	Late Medieval (AD 1425–1475)
9	Oats ( <i>Avena sativa</i> )	30	219.1	Rotterdam-Markthal	128	Peat/dung	51° 55' 12.8"	4° 29' 13.1"	Late Medieval (AD 1300–1425)
10	Hulled barley ( <i>Hordeum vulgare</i> var. <i>vulgare</i> )	30	305.9	Spijkenisse 10.36	180	Peat	51° 51' 33.6"	4° 17' 11.1"	Roman period (12 BC–AD 450)
11	Hulled barley ( <i>Hordeum vulgare</i> var. <i>vulgare</i> )	30	187.6	Boxmeer Maasbroekse blokken	48/022	Sandy loam, podzol	51° 39' 34.4"	5° 56' 0.6"	Middle Bronze Age (1400–1260 BC)
12	Naked barley ( <i>Hordeum vulgare</i> var. <i>nudum</i> )	30	387.5	Wijchen Oosterweg	14	Sand	51° 48' 11.5"	5° 44' 19.1"	Late Neolithic (2500–2000 BC)
13	Pea ( <i>Pisum sativum</i> )	15	193.5	Rotterdam-Markthal	128	Peat/dung	51° 55' 12.8"	4° 29' 13.1"	Late Medieval (AD 1300–1425)
14	Pea ( <i>Pisum sativum</i> )	15	522.2	Maastricht Onze Lieve Vrouwenplein	1/3/7	Loess	50° 50' 50.6"	5° 41' 38.0"	Late Medieval (AD 1200–1400)
15	Celtic bean ( <i>Vicia faba</i> var. <i>minor</i> )	15	1530.1	Valkenburg Kasteel	3	Loess	50° 51' 43.7"	5° 49' 51.2"	Late Medieval (AD 1150–1200)
16	Celtic bean ( <i>Vicia faba</i> var. <i>minor</i> )	15	813.6	Elst-Brienshof	8/2/23	River clay	51° 54' 48.2"	5° 50' 42.1"	Roman period (12 BC–AD 450)
17	Millet ( <i>Panicum miliaceum</i> )	60	97.5	Weerselo-Deurningen	3	Sand	52° 19' 49.8"	6° 48' 13.3"	Iron Age (800–12 BC)
18	Hulled barley ( <i>Hordeum vulgare</i> var. <i>vulgare</i> )	30	265.7	Venray-Hoogriebroek	27/3/36	Sand	51° 30' 25.1"	6° 1' 16.8"	Roman period (12 BC–AD 450)
19	Lentil ( <i>Lens culinaris</i> )	30	162.2	Deventer Colmschate	54/2/5	Sand	52° 14' 58.8"	6° 12' 27.7"	Iron Age (800–12 BC)
20	Oak ( <i>Quercus</i> sp.)	15	1300.9	Deventer Colmschate	61/1/12	Sand	52° 14' 58.8"	6° 12' 27.7"	Early Iron Age (800–500 BC)
21	Oak ( <i>Quercus</i> sp.)	30	4330.4	Amersfoort-Zoicherpad	–	Sand	52° 10' 52.5"	5° 23' 40.3"	Late Iron Age (250–12 BC)
22	Emmer ( <i>Triticum dicoccon</i> )	30	275.4	Bovenkarspel	105/2/1	(Sandy) loam	52° 43' 3.7"	5° 14' 23.8"	Bronze Age (2000–800 BC)

employed with the timing, duration and volume of dilution coded into the measurement method. In order to measure more than one element at a time, a gas configuration change must be performed. This is achieved via a calibration jump utilizing a 'fast magnet switch' that alters the magnetic field from monitoring nitrogen  $N_2$  ( $m/z$  28, 29 and 30) to monitoring carbon as  $CO_2$  ( $m/z$  44, 45 and 46).

Primary reference material (IAEA Reference Materials Group Laboratories, Seibersdorf, Austria) was used as accepted value anchor points in order to calibrate in-house (or internal) laboratory standards. The approach taken for running unknown samples was to run both primary and internal standards, along with the unknown samples which are run in duplicate. Standards are chosen to encompass the range of expected results from unknowns and are

interspersed throughout the run bracketing the unknown samples. The internal precision of the instrument from reference gas pulse determinations is  $\pm 0.070$  for carbon and  $\pm 0.038$  for nitrogen, and from repeated primary and in-house standard measurements, the instrument measurement error from runs of standards was determined to be  $\pm 0.2\%$ , 1 s.d.

Results were reported with respect to Vienna Pee Dee Belemnite for carbon using the SI quantity symbol delta ( $\delta^{13}C$  V-PDB)<sup>32</sup> and for nitrogen with respect to Ambient Inhalable Reservoir (AIR), for example ( $\delta^{15}N$  AIR)  $\delta^{15}N = R_{\text{sample}}/R_{\text{standard}} - 1$  ( $R$  is the ratio of  $^{15}N/^{14}N$ ).<sup>33</sup> The uncertainty ( $1\sigma$ ) of carbon and nitrogen isotope ratio measurements, determined from repeated measurement of international and laboratory standards, was 0.2 and 0.3‰, respectively.

## 2.4 | Attenuated total reflectance FTIR analysis

FTIR spectra of carbonized plant samples were measured using a PerkinElmer (Waltham, MA, USA) Spectrum 100 FTIR spectrometer. Each measurement corresponded to 16 scans made between 4000 and 450  $\text{cm}^{-1}$ . A baseline correction was carried out using the device software and all spectra were normalized to a wavenumber of 4000  $\text{cm}^{-1}$ , which represented, in most cases, the most intense peak. Earlier measurements of charred plant remains revealed that duplicate measurements were not significantly different (Van Hoesel and Braadbaart, unpublished data).

## 2.5 | Portable XRF analysis

Elemental measurements were made using a Thermo Scientific Niton XL3t p-XRF device with a GOLDD+ detector and equipped with a silver anode operating at a maximum of 50 kV and 40  $\mu\text{A}$ . Measurements were performed in a factory-calibrated 'mining mode'. The total measurement time was 110 s using four different settings according to target elements: (Mg, Al, Si, P, S, Cl; 40 s); (Ca, K, Sc, Ti; 20 s); (from Au to Pb in the periodic table; 40 s); (Ag to Au; 10 s). The measured values are externally calibrated using 21 certified soil and sediment powder reference materials (WEPAL; ISE), covering a wide range of grain sizes from sand to fine clay and loess (see supporting information). All measurements were performed under laboratory conditions in an XRF stand with fixed sample positions. Discussed here are only the Ca, Mn and Fe measurements as markers for the presence of carbonate and humic contaminants. The remaining measurements are given in the supporting information.

The performance of p-XRF devices can be greatly influenced by the adoption of an appropriate methodological approach. This includes, for instance, adequate sample preparation and a calibration process relying on internationally recognized standards.<sup>34</sup> For quantitative results the sample should be 'infinitely' thick, completely flat, homogeneous without different mineralogical phases and very fine-grained or amorphous.

For the application presented here to our knowledge no international standards were available. Therefore, the applied calibration scheme (i.e. internal standardization followed by external calibration with international soil samples) will only provide semi-quantitative results.

Charred material (mainly C and H) has a lower X-ray absorption than silicate matrix samples. This effect will be enhanced for thin samples, leading to overestimations of the concentration values for most elements. In order to establish the dependency between sample thickness and apparent elemental concentrations, different amounts of powdered charred plant material were analysed. The amount of sample after which no changes in the elemental composition occurred was ca 500 mg (ca 1 cm thickness). This amount corresponds to ca 100 charred grain kernels or ca 500 millet grains. However, for many cases only ca 30 grains (ca 150 mg) were available for stable isotope analysis. Thus, p-XRF measurements were compared with those obtained from inductively coupled plasma optical emission spectroscopy (ICP-OES) analysis. Given the requirements in amount of material in the latter, this was possible for five samples. Since ICP-OES analysis requires

ash residues, the samples were first ashed using thermogravimetric analysis (TGA), which yielded additional information on the phase composition of the samples.

## 2.6 | TGA

TGA was performed using a LECO (Saint Joseph, MI, USA) TGA 701 automated thermogravimetric analyser to quantify the presence of calcium compounds. From each sample, approximately 1 g of grain material was added to a ceramic crucible. The TGA oven was heated at a rate of 5°C  $\text{min}^{-1}$  until a temperature of 1000°C was reached and maintained for 20 minutes. Weights were recorded automatically at intervals of 4 minutes using an analytical balance. Sample weights were recorded with a precision of 0.1 mg.

## 2.7 | ICP-OES analysis

The elemental composition of the five ash samples resulting from TGA analyses were measured using ICP-OES with a SPECTRO (Kieve, Germany) CIROS CCD ICP spectrometer. The ash samples were totally dissolved using a combination of HF,  $\text{HNO}_3$ ,  $\text{HClO}_4$  and HCl in closed vessels. This was followed by evaporation until incipient dryness in order to remove excess HF and silica as  $\text{SiF}_4$ . The residue was then taken up in 5 mL of concentrated HCl and diluted 10 times.

The measurement precision (<5% Al, As, Be, Ca, Cd, Cr, Fe, Mg, Mn, Na, Ti, Y; 5–10% Ba, Co, Cu, K, Li, Ni, Mo, P, S, Sc, V, Zr; 10–15% Pb, Sr) was determined from repeated analyses of the international soil standard ISE 921. In order to directly compare elemental concentration results obtained from ICP-OES and p-XRF, the measured ICP-OES values were corrected for ash weight loss during the preceding TGA.

# 3 | RESULTS

## 3.1 | Weight loss

The different pre-treatment steps resulted in substantial weight losses (Table 2). Sample weight loss under an A-only pre-treatment averaged  $22 \pm 9\%$  ( $n = 22$ ), and under the BA pre-treatment  $37 \pm 22\%$  ( $n = 21$ ). The total loss for the full ABA was  $50 \pm 17\%$ . Previous studies also reported significant weight losses, but typically larger than the values reported here.<sup>11,16</sup> These differences can be attributed to diverse sample preservation, to the degree of charring or to how specific pre-treatment steps were performed (e.g. decantation, centrifuging speed).

Tests on four samples showed no significant differences in the stability of pre-treated pellet material between two centrifuging speeds (2500 versus 5000 rpm). In this study, the largest sample losses (>90%) were observed for the two smallest samples, both millets, occurring principally during the BA part of the pre-treatment.

## 3.2 | Attenuated total reflectance FTIR results

The observed infrared spectra were similar for the majority of the untreated samples. These were dominated by large peaks at 1570  $\text{cm}^{-1}$  (asymmetric  $\text{COO}^-$  stretching and/or aromatic C=C ring

**TABLE 2** Sample dry weights, FTIR peaks potentially related to contamination, main p-XRF results, weight losses and stable isotope measurements<sup>a</sup> [Color table can be viewed at [wileyonlinelibrary.com](http://wileyonlinelibrary.com)]

Sample no.	Dry weight (mg)	FTIR peaks										p-XRF (%)					Weight loss (%)					Acid-only					ABA								
		Untreated		A-only		A-only		A-only		A-only		A-only		A-only		A-only		A-only		A-only		A-only		A-only		A-only		A-only		A-only		A-only		A-only	
		Untreated	A-only	Fe <sub>2</sub> O <sub>3</sub>	CaO	MnO	MnO	A-only	ABA	δ <sup>15</sup> N (%)	N (%)	δ <sup>13</sup> C (%)	C (%)	Atomic C/N	δ <sup>15</sup> N (%)	N (%)	δ <sup>13</sup> C (%)	C (%)	Atomic C/N	δ <sup>15</sup> N (%)	N (%)	δ <sup>13</sup> C (%)	C (%)	Atomic C/N	δ <sup>15</sup> N (%)	N (%)	δ <sup>13</sup> C (%)	C (%)	Atomic C/N	δ <sup>15</sup> N (%)	N (%)	δ <sup>13</sup> C (%)	C (%)	Atomic C/N	
1	91.4	-	-	2.0	7.3	3.1	3.1	20.5	91.1	7.7*	3.1	-10.3	37.6	16.7	8.7	4.7	-10.3	53.9	15.5	8.7	3.8	-10.8	46.6	16.6	8.7	3.8	-10.8	46.6	16.6	8.7	3.8	-10.8	46.6	16.6	
2	364.6	-	-	6.6	17.2	0.5	0.5	21.7	36.9	6.6	2.9	-23.1	38.6	18.4	6.3	2.9	-23.2	43.5	20.2	7.1	4.2	-23.0	57.2	18.7	7.1	4.2	-23.0	57.2	18.7	7.1	4.2	-23.0	57.2	18.7	
3	206.3	-	-	8.1	20.8	0.8	0.8	31.1	44.6	8.1	3.1	-22.5	42.7	18.8	8.0	4.3	-22.4	58.4	18.4	7.9	4.3	-22.4	61.4	19.4	7.9	4.3	-22.4	61.4	19.4	7.9	4.3	-22.4	61.4	19.4	
4	220.9	-	-	4.4	24.1	0.0	0.0	21.2	70.0	13.6	2.8	-24.9	46.9	22.9	13.6	3.5	-25.1	58.5	22.8	14.3	3.1	-24.9	59.7	26.6	14.3	3.1	-24.9	59.7	26.6	14.3	3.1	-24.9	59.7	26.6	
5	279.9	-	-	0.4	20.6	0.0	0.0	15.3	33.4	3.3	4.0	-21.8	51.0	17.3	3.4	4.8	-21.9	59.9	16.8	3.2	4.6	-21.8	60.9	18.0	3.2	4.6	-21.8	60.9	18.0	3.2	4.6	-21.8	60.9	18.0	
6	435.0	-	-	0.9	21.8	0.1	0.1	26.7	40.8	3.1	2.2	-23.2	43.5	27.0	3.2	2.9	-23.2	54.7	25.8	3.3	3.0	-23.3	57.1	26.3	3.3	3.0	-23.3	57.1	26.3	3.3	3.0	-23.3	57.1	26.3	
7	147.5	-	-	2.7	2.9	1.0	1.0	20.3	42.3	5.5	2.8	-22.8	47.3	22.8	5.7	3.5	-22.7	56.8	22.3	5.5	3.3	-22.6	57.5	23.6	5.5	3.3	-22.6	57.5	23.6	5.5	3.3	-22.6	57.5	23.6	
8	181.6	-	-	0.7	22.9	0.0	0.0	22.4	36.4	5.7	2.7	-22.0	47.4	23.9	5.9	3.4	-22.3	61.6	24.5	5.4	3.4	-22.0	60.7	24.6	5.4	3.4	-22.0	60.7	24.6	5.4	3.4	-22.0	60.7	24.6	
9	219.1	√+ <sup>#</sup>	-	9.1	15.2	0.0	0.0	19.4	43.4	6.6	3.8	-23.9	44.7	16.0	6.7	5.4	-23.7	57.5	14.6	6.7	5.6	-23.7	61.2	14.9	6.7	5.6	-23.7	61.2	14.9	6.7	5.6	-23.7	61.2	14.9	
10	305.9	-	-	7.6	18.9	0.2	0.2	22.3	43.4	6.1	2.2	-23.9	40.7	24.7	6.1	3.0	-24.1	53.8	24.9	6.1	2.4	-24.0	49.8	28.4	6.1	2.4	-24.0	49.8	28.4	6.1	2.4	-24.0	49.8	28.4	
11	187.6	\$@	-	2.7	6.1	0.2	0.2	15.8	49.4	7.7	3.1	-25.0	49.4	21.5	7.7	3.6	-25.0	57.8	21.9	7.7	3.5	-24.9	60.2	23.5	7.7	3.5	-24.9	60.2	23.5	7.7	3.5	-24.9	60.2	23.5	
12	387.5	\$@	-	14.2	6.1	4.5	4.5	20.9	46.7	8.3	2.1	-24.6	32.1	21.0	9.1	2.6	-24.7	42.1	22.3	9.0	3.0	-24.6	53.4	24.5	9.0	3.0	-24.6	53.4	24.5	9.0	3.0	-24.6	53.4	24.5	
13	193.5	√+	-	5.6	13.7	0.0	0.0	20.7	X <sup>b</sup>	2.0	7.7	-25.3	51.6	7.8	1.8	5.3	-25.3	36.5	8.0	X <sup>b</sup>	X <sup>b</sup>	X <sup>b</sup>	X <sup>b</sup>	X <sup>b</sup>	X <sup>b</sup>	X <sup>b</sup>	X <sup>b</sup>	X <sup>b</sup>	X <sup>b</sup>	X <sup>b</sup>	X <sup>b</sup>	X <sup>b</sup>	X <sup>b</sup>	X <sup>b</sup>	X <sup>b</sup>
14	522.2	-	-	1.2	19.4	0.0	0.0	15.6	59.0	1.6	6.5	-25.1	48.6	10.2	1.6	7.9	-25.1	58.7	10.2	1.5	7.6	-24.6	59.7	10.7	1.5	7.6	-24.6	59.7	10.7	1.5	7.6	-24.6	59.7	10.7	
15	1530.1	-	-	0.0	18.3	0.0	0.0	24.2	35.5	1.9	5.6	-24.9	47.2	11.4	1.7	7.2	-24.8	59.4	11.2	1.6	6.6	-24.7	54.3	11.2	1.6	6.6	-24.7	54.3	11.2	1.6	6.6	-24.7	54.3	11.2	
16	813.6	√+ <sup>#</sup>	-	2.4	28.0	1.8	1.8	37.1	53.2	2.8	6.0	-24.2	39.1	8.9	3.0	8.8	-24.2	57.4	8.9	2.7	9.0	-24.4	60.2	9.1	2.7	9.0	-24.4	60.2	9.1	2.7	9.0	-24.4	60.2	9.1	
17	97.5	-	-	19.7	0.4	0.4	0.4	51.9	98.4	7.1	2.1	-11.5	29.4	19.3	8.2*	3.7	-11.0*	44.7	16.5	6.3	2.6	-12.0	34.1	17.9	6.3	2.6	-12.0	34.1	17.9	6.3	2.6	-12.0	34.1	17.9	
18	265.7	\$@	-	2.0	5.0	0.2	0.2	15.9	39.6	6.4	2.6	-24.5	47.8	24.7	6.4	3.0	-24.4	59.7	26.8	6.7	2.9	-24.3	59.4	28.2	6.7	2.9	-24.3	59.4	28.2	6.7	2.9	-24.3	59.4	28.2	
19	162.2	-	-	1.5	22.7	0.0	0.0	14.0	60.4	2.2	7.5	-25.0	49.7	9.0	2.0	8.8	-25.1	58.7	9.1	2.0	8.6	-25.2	59.4	9.5	2.0	8.6	-25.2	59.4	9.5	2.0	8.6	-25.2	59.4	9.5	
20	1300.9	-	-	0.8	6.9	1.2	1.2	16.9	42.7	-0.2	1.8	-25.1	49.3	37.8	-0.4	2.0	-25.1	56.5	38.0	-0.7	2.1	-25.1	61.1	38.7	-0.7	2.1	-25.1	61.1	38.7	2.5	1.8	-23.9	63.5	40.6	
21	4330.4	-	-	0.3	2.1	0.0	0.0	7.7	32.8	2.4	1.5	-23.8	54.6	42.2	1.8	1.7	-23.8	58.8	41.0	2.5	1.8	-23.9	63.5	40.6	2.5	1.8	-23.9	63.5	40.6	2.5	1.8	-23.9	63.5	40.6	
22	275.4	-	-	8.8	14.0	2.0	2.0	27.1	54.8	10.5	3.5	-23.2	37.9	12.5	10.2	4.4	-23.2	47.6	12.6	10.3	4.8	-23.1	53.5	13.0	10.3	4.8	-23.1	53.5	13.0	10.3	4.8	-23.1	53.5	13.0	

<sup>a</sup>Symbols for FTIR peaks (cm<sup>-1</sup>): √ = 1085 (nitrite); + = 1460 (nitrite); # = 870 (carbonate); ? = 870? (carbonate); \$ = 1010 (humic acid); @ = 1080 (humic acid). Asterisks in isotopic values identify statistically significant differences (Z-score test) towards ABA values.<sup>b</sup>The ABA residue of sample 13 was lost during weighing.



stretching),  $1375\text{ cm}^{-1}$  (symmetric  $\text{COO}^-$  stretching and/or aliphatic  $\text{CH}_3$  deformation) and, in approximately half the samples, also at  $1030\text{ cm}^{-1}$  (C–O stretching) (Figure 1). After both pre-treatments, the peak at  $1570\text{ cm}^{-1}$  was shifted to larger wavelengths ( $1595\text{ cm}^{-1}$ ) and a small new peak at  $1700\text{ cm}^{-1}$  (aromatic C=O stretching) appeared on its shoulder. In addition a large peak near  $1220\text{ cm}^{-1}$  (aromatic C–O stretching and phenolic OH deformation of COOH) became visible. All these bonds are common in moieties from charred plant material.<sup>35</sup> These peaks have also been observed and identified earlier.<sup>11,14</sup> After pre-treatment, the broad peak at  $1375\text{ cm}^{-1}$  disappeared, often leaving a small double peak at  $1430\text{ cm}^{-1}$  (aromatic C=C ring stretching) and  $1370\text{ cm}^{-1}$  (Figure 1). These changes may be ascribed to the disassociation of carboxylate ions, during the acid step, from contaminating metal ions taken up from the surrounding soil.<sup>36</sup> The FTIR spectra of the ABA pre-treated samples showed no additional changes from those of the A-only samples.

To identify possible contamination, we compared the FTIR spectra of our samples with those of Vaiglova et al who artificially contaminated their samples with carbonates, nitrates and humic acid. The infrared spectra showed no clear indications for the presence of carbonates or nitrites. However, these contaminants are only visible in the FTIR spectra in concentrations above 5–10%.<sup>11</sup>

Sample 16, and to a lesser degree sample 9, furthermore showed a small peak at  $870\text{ cm}^{-1}$  ( $\text{CO}_3^{2-}$   $\nu_2$  deformation) which might indicate carbonate contamination. Considering the low intensity of this peak, it is possible that the smaller carbonate peak at  $720\text{ cm}^{-1}$  ( $\nu_4$  in-plane bending) remained invisible. However, these two samples also contained a double peak at  $600$  and  $560\text{ cm}^{-1}$ . The combination of peaks at  $870$ ,  $600$  and  $560\text{ cm}^{-1}$  can be related to the presence of phosphate, which also has an intense peak at  $1030\text{ cm}^{-1}$  ( $\nu_3$  phosphate asymmetric stretch).<sup>37,38</sup> These peaks disappear as a result of the acid-only and ABA pre-treatments. Samples 11, 12 and 18

showed small 'peaks' at  $1080$  and  $1010\text{ cm}^{-1}$ , but lack the third humic acid diagnostic peak at  $3690\text{ cm}^{-1}$  reported previously.<sup>11</sup> These two peaks were not affected by the acid-only pre-treatment but disappeared after the ABA pre-treatment, which would be expected for humic acids.

### 3.3 | p-XRF elemental results

For 14 untreated samples the concentration of calcium, expressed as CaO, was above 10% (see Table 2). All samples from non-sandy areas had high CaO concentrations while the opposite was observed for samples from sandy soils (Figure 2). The exception to the latter was sample 19, a lentil sample originating from a sandy soil that showed high CaO concentrations.

All five pulses had CaO concentrations larger than 14% whereas cereals and acorns showed a larger variability. Iron (Fe), expressed as  $\text{Fe}_2\text{O}_3$ , was present in concentrations larger than 8% in five samples from different soil types (two sandy, one peat/dung, two marine clay). The two samples with the highest Fe concentrations yielded a brownish powder, not observed in any of the other samples. None of the pulses had  $\text{Fe}_2\text{O}_3$  concentrations larger than 6%. Samples 1 and 17, both millets, showed particularly elevated concentrations of MnO and  $\text{Fe}_2\text{O}_3$ , respectively, and both elements were elevated in sample 12.

### 3.4 | Comparison of TGA, ICP-OES and XRF results

The concentration of ash residues measured using TGA varied between 7 and 19% (Table 3). The TGA weight loss analysis did not show distinct peaks that can be attributed to compounds other than charred organic matter and in samples 5 and 6 to  $\text{CaCO}_3$ .

A comparison between CaO concentrations measured using ICP-OES and p-XRF showed that the latter typically leads to an overestimation by *ca* 1% (Table 1). The exception is sample 5 where

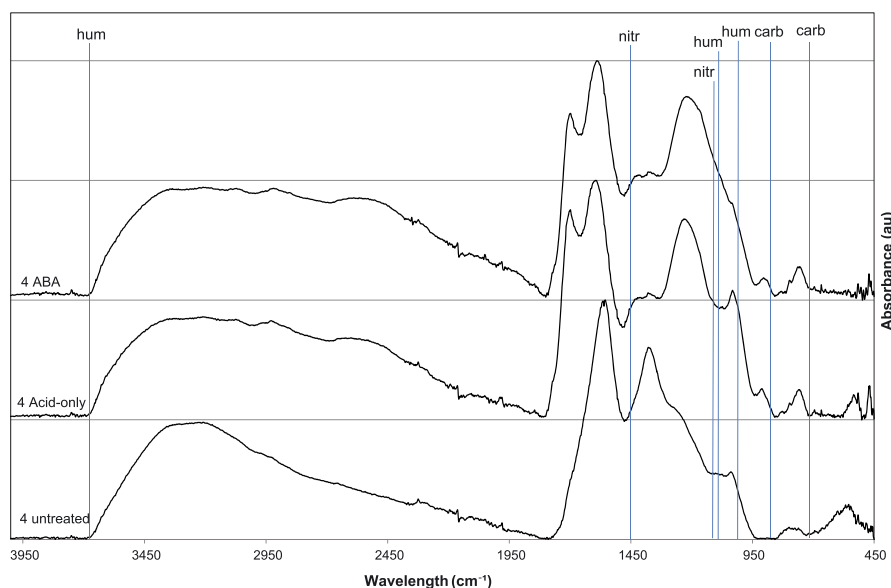


**FIGURE 1** Typical FTIR spectra obtained for charred plant samples (no. 4): Untreated, acid-only treated and acid–base–acid treated; hum = wavelengths of humic acid peaks, nitr = wavelengths of nitrite peaks, carb = wavelengths of carbonate peaks, all contaminant wavelengths according to Vaiglova et al<sup>11</sup> [Color figure can be viewed at [wileyonlinelibrary.com](http://wileyonlinelibrary.com)]

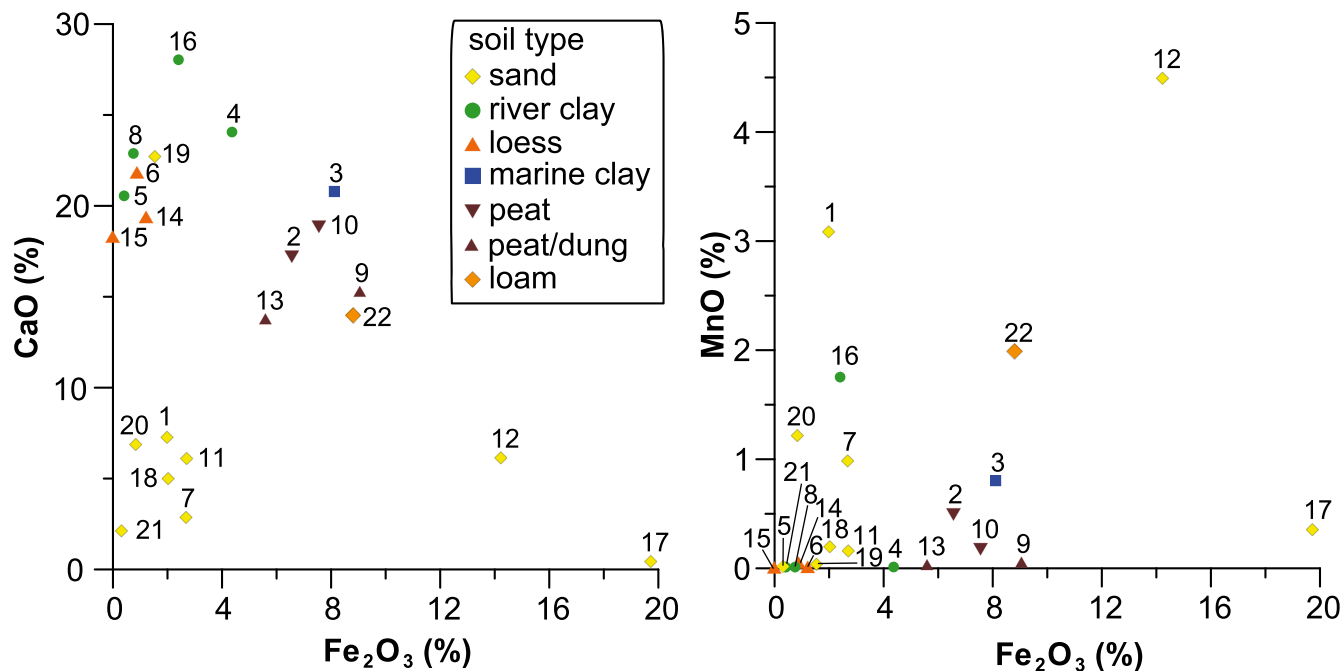


**FIGURE 2** Scatterplots of elemental concentrations measured for untreated samples using p-XRF showing  $\text{Fe}_2\text{O}_3$  versus CaO (left) and  $\text{Fe}_2\text{O}_3$  versus MnO (right) and classified according to soil type [Color figure can be viewed at [wileyonlinelibrary.com](http://wileyonlinelibrary.com)]

the CaO overestimation was 8%; this outlier probably illustrates the semi-quantitative value of the p-XRF measurements. The  $\text{Fe}_2\text{O}_3$  and MnO concentration values were slightly overestimated by p-XRF compared with the ICP-OES results by *ca* 0.2 and 0.02%, respectively. The exception to the latter was sample 7.

### 3.5 | Stable isotope results

Stable isotope measurements for the various sample pre-treatments are listed in Table 2. Figure 3 shows the  $\delta^{13}\text{C}$  offsets ( $\Delta^{13}\text{C}$ ) of untreated and A-only pre-treated towards the ABA pre-treated values, which were taken as reference for the uncontaminated signal. A Z-score test showed significant differences towards ABA  $\delta^{13}\text{C}$  values only for acid-treated sample 17. The largest offsets occur for samples 1, 14 and 17 which are among those that had the largest mass losses following pre-treatment (Table 2). Samples 1 and 17 are both millet samples with the smallest available sample weights, although the weight of the material taken for isotopic measurements was similar to that of other samples. None of the  $\Delta^{13}\text{C}$  offset values exceeded 1‰ and the vast majority did not exceed 0.5‰.

**TABLE 3** Ash content and XRF and ICP measurements (CaO,  $\text{Fe}_2\text{O}_3$  and MnO) on untreated samples

Sample	Ash (%)	CaO (%)		$\text{Fe}_2\text{O}_3$ (%)		MnO (%)	
		p-XRF	ICP-OES	p-XRF	ICP-OES	p-XRF	ICP-OES
5	11	21	13	0.41	0.2	0.01	0.03
6	19	22	21	0.88	0.31	0.05	0.04
7	14	2.9	0.9	2.68	0.84	0.98	0.36
21	7	2.1	1.7	0.31	0.25	0.02	0.04
Test sample	13	6.8	5.2	0.87	0.53	0.16	0.12

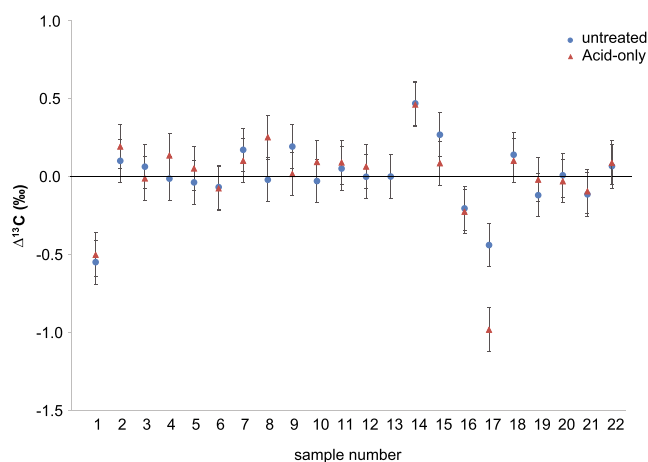


**FIGURE 3**  $\delta^{13}\text{C}$  offsets ( $\Delta^{13}\text{C}$ ) of untreated and A-only pre-treated towards the ABA pre-treated samples. For sample 13, the offset of untreated towards A-only pre-treated is given due to the lack of an ABA measurement [Color figure can be viewed at [wileyonlinelibrary.com](http://wileyonlinelibrary.com)]

Figure 4 shows the  $\delta^{15}\text{N}$  offset ( $\Delta^{15}\text{N}$ ) for untreated and A-only towards ABA. All the  $\Delta^{15}\text{N}$  values are within 1‰, except for A-only in sample 17 (−1.93‰). A Z-score test showed significant differences towards ABA  $\delta^{15}\text{N}$  values for untreated sample 1 and for acid-treated sample 17. As with  $\Delta^{13}\text{C}$ , both millet samples show the largest  $\Delta^{15}\text{N}$  values. For the untreated samples, samples 1, 4 and 12 have positive  $\Delta^{15}\text{N}$  values while  $\Delta^{15}\text{N}$  was negative for sample 17. For A-only, the offsets for sample 2 and 4 are positive, and for sample 17 negative.

The isotopic offsets between the ABA and untreated samples followed approximately symmetric distributions (Figures 5A and 5B) both for  $\delta^{13}\text{C}$  ( $\Delta^{13}\text{C}_{\text{average}} = 0 \pm 0.4\text{‰}$ ) and  $\delta^{15}\text{N}$  ( $\Delta^{15}\text{N}_{\text{average}} = 0 \pm 0.2\text{‰}$ ). There were no significant differences between ABA and untreated values for either  $\delta^{13}\text{C}$  (paired Welch two sample t-test:  $t =$

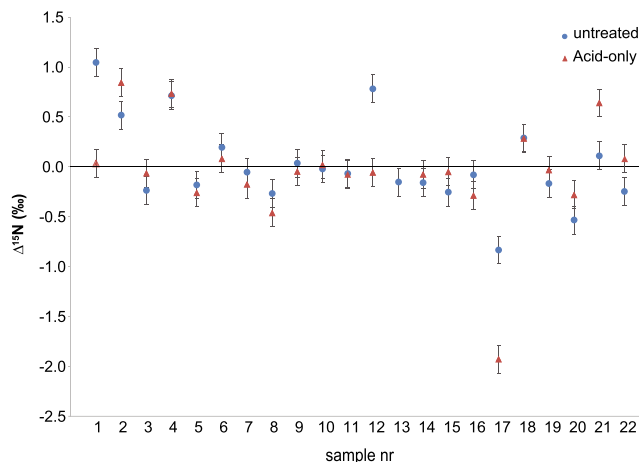


**FIGURE 4**  $\delta^{15}\text{N}$  offset ( $\Delta^{15}\text{N}$ ) between (averaged) untreated and A-only towards (averaged) ABA pre-treated samples. For sample 13, the offset between untreated and A-only pre-treated is given due to lack of an ABA measurement [Color figure can be viewed at wileyonlinelibrary.com]

0,  $df = 20$ ,  $p$ -value = 1) or  $\delta^{15}\text{N}$  (paired Welch two sample  $t$ -test:  $t = -0.41323$ ,  $df = 20$ ,  $p$ -value = 0.6838). The isotopic offsets between ABA and A-only treated samples also followed approximately symmetric distributions (Figure 5A,B) both for  $\delta^{13}\text{C}$  ( $\Delta^{13}\text{C}_{\text{average}} = 0 \pm 0.3\text{‰}$ ) and  $\delta^{15}\text{N}$  ( $\Delta^{15}\text{N}_{\text{average}} = 0.1 \pm 0.5\text{‰}$ ). There were no significant differences between the ABA and A-only values for either  $\delta^{13}\text{C}$  ( $t = 0$ ,  $df = 20$ ,  $p$ -value = 1) or  $\delta^{15}\text{N}$  (paired Welch two sample  $t$ -test:  $t = 0.4445$ ,  $df = 20$ ,  $p$ -value = 0.6615).

Sample 12 is exceptional given that a large amount of sediment was attached to the charred grains (Figure 6). This seems to have occurred before or during the moment of deposition, and not as contamination during burial. This sample showed the highest Mn concentration value and it also had a high Fe concentration.



**FIGURE 6** Stereomicroscope photo of naked barley grains from sample 12 clearly showing traces of sediments attached to the grains during charring [Color figure can be viewed at wileyonlinelibrary.com]

The highest carbon concentration values (*ca* 50%) were observed for two acorn samples (20 and 21) while the lowest were observed for samples 12 (barley with attached sediment) and 17 (millet) (32 and 29%, respectively). Following pre-treatment, the carbon concentrations in cereals rise (Figure 5C). Sample 17 had the lowest carbon concentration of all the untreated samples (29.3%), increasing to 47.2% after acid-only pre-treatment but decreasing to 34.1% after ABA pre-treatment.

The nitrogen concentrations were *ca* 3% for the untreated samples of cereals (mean  $2.9 \pm 0.6\%$ ; Figure 5D), mean  $1.6 \pm 0.1\%$  for the two acorns and  $6.7 \pm 0.8\%$  for pulses. Following pre-treatment, these concentrations increased by *ca* 0.5–1% for cereals and pulses, while both acorns showed no significant influence of pre-treatment. Increases in carbon and nitrogen concentrations, also previously observed,<sup>8</sup> indicate that there was a substantial amount of carbon- and nitrogen-free material removed during the pre-treatments.

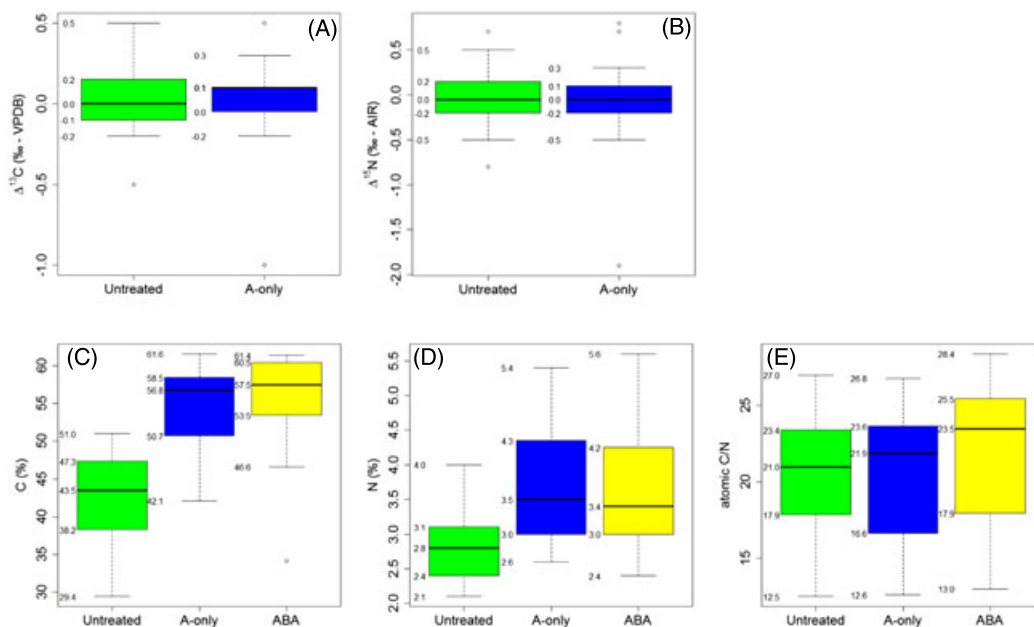


**FIGURE 5** Boxplots showing (A) distribution of  $\Delta^{15}\text{N}$  values for all samples, (B) distribution of  $\Delta^{13}\text{C}$  values for all samples, (C) distribution of C (%) values for cereals, (D) distribution of N (%) values for cereals, (E) distribution of atomic C/N values for cereals. Box edges represent 25th and 75th percentiles (inter quartile range or IQR) while the horizontal line is the 50th percentile (median). Whiskers are the minimum and maximum values that do not exceed a distance of 1.5 times the IQR. Beyond this distance single points represent outliers [Color figure can be viewed at wileyonlinelibrary.com]



The average atomic C/N values according to species following ABA pre-treatment were:  $10.1 \pm 1.0$  ( $n = 4$ ) for pulses,  $43.1 \pm 6.1$  ( $n = 2$ ) for acorns and  $21.7 \pm 4.7$  ( $n = 15$ ) for cereals (Figure 5E). A comparison of mean atomic C/N values between ABA and untreated ( $9.9 \pm 1.2$  for pulses,  $43.5 \pm 8.1$  for acorns and  $20.6 \pm 3.7$  for cereals) or A-only ( $9.8 \pm 1.1$  for pulses,  $42.9 \pm 6.9$  for acorns and  $20.5 \pm 4.2$  for cereals) samples shows that the differences were comparatively small.

## 4 | DISCUSSION

The observed differences between the isotopic ratios of pre-treated and untreated archaeological samples are in overall agreement with previous studies.<sup>8,11,21</sup> Combined data of current and previous studies show that for the vast majority of cases the largest expectable isotopic offsets between untreated and treated samples are smaller than 1‰ for  $\delta^{13}\text{C}$  values and 1.5‰ for  $\delta^{15}\text{N}$  values. If these extreme values are taken as references, then reliable results can be provided by employing  $1\sigma$  (68%) uncertainty values of 0.4 and 0.6‰ for  $\delta^{13}\text{C}$  and  $\delta^{15}\text{N}$  values, respectively. These uncertainty values are conservative for the samples described in the present study and measurement uncertainties can be employed instead.

The overall agreement among  $\delta^{13}\text{C}$  values of untreated and pre-treated samples was observed in spite of the large diversity of burial conditions and the potential presence of contaminants suggested by elemental measurements. Elemental p-XRF measurements showed that 13 samples had Ca concentrations, expressed as CaO, larger than 10%. These high levels of Ca could be associated with the presence of precipitated exogenous calcium carbonate ( $\text{CaCO}_3$ ). However, carbonate concentrations above 10% were not detected by FTIR analysis, except for samples 16 and 9.<sup>11</sup> This suggests that the Ca compounds present in charred material were carbon-free (e.g. calcium oxide) or that, at least partially, the carbon may originate from endogenous calcium compounds. Possible endogenous Ca sources are calcium oxalate and calcium phytate having  $\delta^{13}\text{C}$  values similar to those of bulk plant material.<sup>20</sup> During charring, phytate is probably converted to smaller moieties still binding Ca, probably to phosphate- or carbonate-containing compounds. The source of carbon for these Ca compounds would include  $\text{HCO}_3^-$  from degraded endogenous plant material. This would be in agreement with previous studies showing that highly carboxylated and aromatic alkali-extractable humic acids in archaeological charcoals are mainly produced from diagenetic alterations and during charring of endogenous plant material.<sup>30</sup> The  $\delta^{13}\text{C}$  values for groundwater dissolved inorganic carbon are unknown for the sample sites. However,  $\delta^{13}\text{C}$  values for dissolved inorganic carbon are dominated by the decay of organic matter and for predominately C3 environments should range between *ca* -20 and -25‰, approaching original plant values for most samples listed here.<sup>28</sup>

The  $\delta^{15}\text{N}$  offsets ( $\Delta^{15}\text{N}$ ) of untreated and A-only compared with ABA values are mostly within 0.5‰ indicating a predominately endogenous origin for nitrogen. However, the agreement among the  $\delta^{15}\text{N}$  values of untreated and pre-treated samples was not as good as that observed for  $\delta^{13}\text{C}$  values. Some samples show  $\Delta^{15}\text{N}$  values up to *ca* 1‰, and sample 17 *ca* 2‰. The two samples that showed the largest  $\Delta^{15}\text{N}$  values were both millets (samples 1 and 17) that, as mentioned previously, also had comparatively large  $\Delta^{13}\text{C}$  values and

the largest weight losses following ABA pre-treatment (>90%). Millets have smaller grain sizes than other cereal grains and thus a larger surface-to-volume ratio, making them more sensitive to external contamination. Sample 12 also showed a significant difference between untreated and ABA pre-treated  $\delta^{15}\text{N}$  values. However, this sample was visibly contaminated by soil particles (Figure 5). Nitrate is an unlikely candidate as a potential source of contamination given that nitrate salts are highly soluble and, if originally present, were likely to have been removed during water sieving and washing preceding the archaeobotanical analyses. Fulvic acids are soluble in acidic solutions but have considerably lower molecular weights than humic acids and large isotopic differences between humic and fulvic acids are not expected.<sup>39</sup> Nitrogen or carbon isotopic differences among treated and untreated samples could also arise from unknown selective leaching of material having significantly different isotopic signals.<sup>4,40,41</sup> However, previous experimental work on charred cereals showed no isotopic indication that selective leaching occurs during ABA pre-treatment.<sup>8</sup>

Comparison of the FTIR peaks for the different pre-treatments shows that the acid step effectively removed any carbonate present in the untreated sample and that the ABA pre-treatment removed both carbonates and humic acids (no humic or carbonate peaks observed following ABA). When considering only the highest isotopic differences among untreated and ABA-treated samples (samples 1, 4, 12, 17), FTIR analysis only detected the presence of humic acids for sample 12. It is important to notice that reference humic acid peaks are based on the experimental work by Vaiglova et al and as such may not include all diagnostic humic acid peaks.<sup>11</sup> Nonetheless, the samples with highest isotopic differences had concentration of either Mn or Fe, or of both elements, above 2%. Humic acids take up and redeposit iron or manganese in the soil; thus, higher concentrations of these elements are potentially indicative of the presence of humic acid contaminants.<sup>42</sup> However, both FTIR and p-XRF analyses showed the presence of potential contaminants without any significant differences among untreated and pre-treated material. As mentioned previously this probably suggests that the magnitude of isotopic differences between endogenous and foreign materials was relatively small or that much of the degraded material is of endogenous origin. Endogenous humic acid compounds within grains would probably also accumulate iron and manganese. Neither p-XRF nor FTIR measurements provided straightforward criteria for detecting a contamination impact. Nonetheless, p-XRF measurements of Fe and Mn were more efficient than FTIR at detecting true positives probably because of the comparatively high detection limits for FTIR.

## 5 | CONCLUSIONS

Isotopic measurements of untreated charred plant samples can offer reliable results provided that different parameters (species, soil types, deposition times and contamination levels) are similar to the wide range described in this study. The use of untreated sample material will greatly increase sample throughput, reduce operational costs and reduce sample needs. However, standard protocols in terms of visual inspection to identify the presence of possible soil contaminants and thorough washing (usually done to extract the charred material from

soil samples) should still be applied. Furthermore, if sample conditions deviate considerably from those described here it is recommended that a comparable study be undertaken, e.g. on a sample subset, to assess the magnitude of the isotopic offset values between treated and untreated samples. Alternatively, a conservative approach may also be taken by reporting larger uncertainties. In view of obtained and previously reported isotopic results, we recommend using  $1\sigma$  (68%) uncertainties for reported isotopic ratios of 0.4 and 0.6‰ for  $\delta^{13}\text{C}$  and  $\delta^{15}\text{N}$  values, respectively.

If the reporting of smaller measurement uncertainties is necessary, an A-only or complete ABA pre-treatment can be applied. The decision to apply these pre-treatments may be based on elemental measurements to assess the presence of exogenous carbonates and humic acids. Large concentrations of characteristic elements (e.g. Ca, Fe, Mn) do not necessarily imply significant offsets between measurement and pre-burial isotopic values. However, this study demonstrated that when larger offsets are observed these are associated with characteristic elemental signatures. In this respect, p-XRF, albeit semi-quantitative, offered a more effective approach than FTIR to the detection of possible diagenetic changes in isotopic values.

## ACKNOWLEDGEMENTS

We are grateful to Merit Hondelink for her assistance in the pre-treatment of the samples, to Carl Heron, Andy Gledhill, Marise Gorton and Julia Beaumont for isotopic measurements and for information on the isotope ratio mass spectrometry method, and to Corrie Bakels and Mans Schepers for useful discussions of our data. The paper further benefitted from the feedback of four anonymous reviewers.

## ORCID

O. Brinkkemper  <http://orcid.org/0000-0003-3126-8459>

## REFERENCES

- Fiorentino G, Ferrio J, Bogaard A, Arais J, Riehl S. Stable isotopes in archaeobotanical research. *Veg Hist Archaeobot*. 2015;24(1):215-227. <https://doi.org/10.1007/s00334-014-0492-9>
- Marino BD, Deniro MJ. Isotopic analysis of archaeobotanicals to reconstruct past climates: Effects of activities associated with food preparation on carbon, hydrogen and oxygen isotope ratios of plant cellulose. *J Archaeol Sci*. 1987;14(5):537-548. [https://doi.org/10.1016/0305-4403\(87\)90037-9](https://doi.org/10.1016/0305-4403(87)90037-9)
- Arais JL, Febrero A, Buxo R, et al. Changes in carbon isotope discrimination in grain cereals from different regions of the western Mediterranean Basin during the past seven millennia. Palaeoenvironmental evidence of a differential change in aridity during the late Holocene. *Glob Chang Biol*. 1997;3(2):107-118. <https://doi.org/10.1046/j.1365-2486.1997.00056.x>
- Bogaard A, Heaton THE, Poulton P, Merbach I. The impact of manuring on nitrogen isotope ratios in cereals: Archaeological implications for reconstruction of diet and crop management practices. *J Archaeol Sci*. 2007;34(3):335-343. <https://doi.org/10.1016/j.jas.2006.04.009>
- Aguilera M, Arais JL, Voltas J, et al. Stable carbon and nitrogen isotopes and quality traits of fossil cereal grains provide clues on sustainability at the beginnings of Mediterranean agriculture. *Rapid Commun Mass Spectrom*. 2008;22(11):1653-1663. <https://doi.org/10.1002/rcm.3501>
- Fernandes R, Grootes P, Nadeau MJ, Nehlich O. Quantitative diet reconstruction of a Neolithic population using a Bayesian mixing model (FRUITS): The case study of Ostorf (Germany). *Am J Phys Anthropol*. 2015;158(2):325-340. <https://doi.org/10.1002/ajpa.22788>
- Kanstrup M, Thomsen IK, Mikkelsen PH, Christensen BT. Impact of charring on cereal grain characteristics: Linking prehistoric manuring practice to  $\delta^{15}\text{N}$  signatures in archaeobotanical material. *J Archaeol Sci*. 2012;39(7):2533-2540. <https://doi.org/10.1016/j.jas.2012.03.007>
- Fraser RA, Bogaard A, Charles M, et al. Assessing natural variation and the effects of charring, burial and pre-treatment on the stable carbon and nitrogen isotope values of archaeobotanical cereals and pulses. *J Archaeol Sci*. 2013;40(12):4754-4766. <https://doi.org/10.1016/j.jas.2013.01.032>
- Nitsch EK, Charles M, Bogaard A. Calculating a statistically robust  $\delta^{13}\text{C}$  and  $\delta^{15}\text{N}$  offset for charred cereal and pulse seeds. *Sci Technol Archaeol Res*. 2015;1(1):1-8. <https://doi.org/10.1179/2054892315Y.0000000001>
- DeNiro MJ, Hastorf CA. Alteration of  $^{15}\text{N}/^{14}\text{N}$  and  $^{13}\text{C}/^{12}\text{C}$  ratios of plant matter during the initial stages of diagenesis: Studies utilizing archaeological specimens from Peru. *Geochim Cosmochim Acta*. 1985;49(1):97-115. [https://doi.org/10.1016/0016-7037\(85\)90194-2](https://doi.org/10.1016/0016-7037(85)90194-2)
- Vaiglova P, Snoeck C, Nitsch E, Bogaard A, Lee-Thorp J. Impact of contamination and pre-treatment on stable carbon and nitrogen isotopic composition of charred plant remains. *Rapid Commun Mass Spectrom*. 2014;28(23):2497-2510. <https://doi.org/10.1002/rcm.7044>
- Tieszen LL. Natural variations in the carbon isotope values of plants: Implications for archaeology, ecology, and paleoecology. *J Archaeol Sci*. 1991;18(3):227-248. [https://doi.org/10.1016/0305-4403\(91\)90063-U](https://doi.org/10.1016/0305-4403(91)90063-U)
- Styring AK, Fraser RA, Arbogast R-M, et al. Refining human palaeodietary reconstruction using amino acid  $\delta^{15}\text{N}$  values of plants, animals and humans. *J Archaeol Sci*. 2015;53:504-515. <https://doi.org/10.1016/j.jas.2014.11.009>
- Styring AK, Manning H, Fraser RA, et al. The effect of charring and burial on the biochemical composition of cereal grains: Investigating the integrity of archaeological plant material. *J Archaeol Sci*. 2013;40(12):4767-4779. <https://doi.org/10.1016/j.jas.2013.03.024>
- Hatte C, Morvan J, Noury C, Paterne M. Is classical acid-alkali-acid treatment responsible for contamination? An alternative proposition. *Radiocarbon*. 2001;43(2A):177-182. <https://doi.org/10.1017/S003382220003798X>
- Kanstrup M, Holst MK, Jensen PM, Thomsen IK, Christensen BT. Searching for long-term trends in prehistoric manuring practice.  $\delta^{15}\text{N}$  analyses of charred cereal grains from the 4th to the 1st millennium BC. *J Archaeol Sci*. 2014;51:115-125. <https://doi.org/10.1016/j.jas.2013.04.018>
- Bird MI, Ayliffe LK, Fifield LK, Turney CSM. Radiocarbon dating of 'old' charcoal using a wet oxidation, stepped-combustion procedure. *Radiocarbon*. 1999;41(2):127-140. <https://doi.org/10.1017/S0033822200019482>
- Southon JR, Magana AL. A comparison of cellulose extraction and ABA pretreatment methods for AMS  $^{14}\text{C}$  dating of ancient wood. *Radiocarbon*. 2010;52(2-3):1371-1379. <https://doi.org/10.1017/S0033822200046452>
- Santos GM, Ormsby K. Behavioral variability in ABA chemical pretreatment close to the  $^{14}\text{C}$  age limit. *Radiocarbon*. 2013;55(2-3):534-544. <https://doi.org/10.1017/S0033822200057660>
- Raven JA, Griffiths H, Glidewell SM, Preston T. The mechanism of oxalate biosynthesis in higher plants: Investigations with stable isotopes  $^{18}\text{O}$  and  $^{13}\text{C}$ . *Proc R Soc Lond Ser B Biol Sci*. 1982;216(1202):87-101.
- Lightfoot E, Stevens RE. Stable isotope investigations of charred barley (*Hordeum vulgare*) and wheat (*Triticum spelta*) grains from Danebury Hillfort: Implications for palaeodietary reconstructions. *J Archaeol Sci*. 2012;39(3):656-662. <https://doi.org/10.1016/j.jas.2011.10.026>
- Styring A, Maier U, Stephan E, Schlichtherle H, Bogaard A. Cultivation of choice: new insights into farming practices at Neolithic lakeshore sites. *Antiquity*. 2016;90(349):95-110. <https://doi.org/10.15184/ajq.2015.192>

23. Styring AK, Charles M, Fantone F, et al. Isotope evidence for agricultural extensification reveals how the world's first cities were fed. *Nat Plants*. 2017;3:1-11. <https://doi.org/10.1038/nplants.2017.76>
24. Styring A, Rösch M, Stephan E, et al. Centralisation and long-term change in farming regimes: Comparing agricultural practices in Neolithic and iron age south-west Germany. *Proc Prehist Soc*. 2017;83:357-381. <https://doi.org/10.1017/ppr.2017.3>
25. Nitsch E, Andreou S, Creuzieux A, et al. A bottom-up view of food surplus: Using stable carbon and nitrogen isotope analysis to investigate agricultural strategies and diet at Bronze Age Archontiko and Thessaloniki Tomba, northern Greece. *World Archaeol*. 2017;49(1):105-137. <https://doi.org/10.1080/00438243.2016.1271745>
26. Heaton THE, Jones G, Halstead P, Tsipopoulos T. Variations in the  $^{13}\text{C}/^{12}\text{C}$  ratios of modern wheat grain, and implications for interpreting data from Bronze Age Assiros Tomba, Greece. *J Archaeol Sci*. 2009;36(10):2224-2233. <https://doi.org/10.1016/j.jas.2009.06.007>
27. Masi A, Sadori L, Balossi Restelli F, Baneschi I, Zanchetta G. Stable carbon isotope analysis as a crop management indicator at Arslantepe (Malatya, Turkey) during the Late Chalcolithic and Early Bronze Age. *Veg Hist Archaeobot*. 2014;23(6):751-760. <https://doi.org/10.1007/s00334-013-0421-3>
28. Cerling TE, Quade J. Stable carbon and oxygen isotopes in soil carbonates. In: Swart PK, Lohmann KC, Kckenzie J, Savin S, eds *Climate Change in Continental Isotopic Records* Washington, DC: American Geophysical Union; 1993:217-231. <https://doi.org/10.1029/GM078p0217>
29. Katsumi N, Yonebayashi K, Fujitake N, Okazaki M. Relationship between stable carbon and nitrogen isotope ratios of humic acids extracted from Andisols and non-Andisols. *Catena*. 2015;127:214-221. <https://doi.org/10.1016/j.catena.2015.01.005>
30. Ascough PL, Bird MI, Francis SM, Lebl T. Alkali extraction of archaeological and geological charcoal: Evidence for diagenetic degradation and formation of humic acids. *J Archaeol Sci*. 2011;38(1):69-78. <https://doi.org/10.1016/j.jas.2010.08.011>
31. van Haaster H, Brinkkemper O. RADAR, a relational archaeobotanical database for advanced research. *Veg Hist Archaeobot*. 1995;4(2):117-125. <https://doi.org/10.1007/BF00206920>
32. Brand WA. New reporting guidelines for stable isotopes - An announcement to isotope users. *Isotopes Environ Health Stud*. 2011;47(4):535-536. <https://doi.org/10.1080/10256016.2011.645702>
33. Coplen TB. Guidelines and recommended terms for expression of stable-isotope-ratio and gas-ratio measurement results. *Rapid Commun Mass Spectrom*. 2011;25(17):2538-2560. <https://doi.org/10.1002/rcm.5129>
34. Kaiser A, Shugar B. Glass analysis utilising handheld Xray fluorescence. In: Shugar JL, Mass AN, eds. *Handheld XRF for Art and Archaeology*. Leuven: Leuven University Press; 2012:449-470
35. Braadbaart F. Carbonization of peas and wheat: a window into the past; a laboratory study. *PhD thesis*, Heemstede, Gravé: Leiden University; 2004
36. Bogaard A, Fraser R, Heaton THE, et al. Crop manuring and intensive land management by Europe's first farmers. *Proc Natl Acad Sci U S A*. 2013;110(31):12589-12594. <https://doi.org/10.1073/pnas.1305918110>
37. Ooi CY, Hamdi M, Ramesh S. Properties of hydroxyapatite produced by annealing of bovine bone. *Ceram Int*. 2007;33(7):1171-1177. <https://doi.org/10.1016/j.ceramint.2006.04.001>
38. Ślósarczyk A, Paszkiewicz Z, Paluszkiwicz C. FTIR and XRD evaluation of carbonated hydroxyapatite powders synthesized by wet methods. *J Mol Struct*. 2005;744-747:657-661. <https://doi.org/10.1016/j.molstruc.2004.11.078>
39. Agnelli A, Bol R, Trumbore SE, Dixon L, Cocco S, Corti G. Carbon and nitrogen in soil and vine roots in harrowed and grass-covered vineyards. *Agric Ecosyst Environ*. 2014;193:70-82. <https://doi.org/10.1016/j.agee.2014.04.023>
40. Hobbie EA, Werner RA. Intramolecular, compound-specific, and bulk carbon isotope patterns in  $\text{C}_3$  and  $\text{C}_4$  plants: A review and synthesis. *New Phytol*. 2004;161:371-385. <https://doi.org/10.1111/j.1469-8137.2004.00970.x>
41. Evans RD. Physiological mechanisms influencing plant nitrogen isotope composition. *Trends Plant Sci*. 2001;6(3):121-126. [https://doi.org/10.1016/S1360-1385\(01\)01889-1](https://doi.org/10.1016/S1360-1385(01)01889-1)
42. Buurman AG, Jongmans P. Podzolisation and soil  $\delta^{15}\text{N}$  dynamics. *Geoderma*. 2005;125:71-83. <https://doi.org/10.1016/j.geoderma.2004.07.006>

## SUPPORTING INFORMATION

Additional Supporting Information may be found online in the supporting information tab for this article.

**How to cite this article:** Brinkkemper O, Braadbaart F, van Os B, van Hoesel A, van Brussel AAN, Fernandes R. Effectiveness of different pre-treatments in recovering pre-burial isotopic ratios of charred plants. *Rapid Commun Mass Spectrom*. 2018;32:251-261. <https://doi.org/10.1016/10.1002/rcm.8033>